

RESONANT RF ELECTROMAGNETIC FIELD INPUT IN THE HELICON PLASMA ION SOURCE

O. V. Alexenko, V. I. Miroshnichenko, S. N. Mordik*

Institute of Applied Physics NAN, Sumy, Ukraine

(Received March 24, 2014)

Spatial distribution of RF electromagnetic field absorption by a plasma electron subsystem of ion source is studied. An ion source operates in a helicon mode ($w_{ci} < w < w_{ce} < w_{pe}$). A simplified model of plasma RF source is used for investigations. Calculations were performed for two particular geometrical dimensions of a discharge chamber with the assumption of two symmetrical modes excitation at two different pressure values of plasma forming gas (helium, hydrogen). The ion source injector parameters of IAP NASU nuclear scanning microprobe were taken for calculations. The calculations show a resonant behaviour of integral RF power absorption as a function of the external magnetic field at a fixed plasma density. Sharpness of resonances becomes smaller as plasma forming gas pressure grows. There is a distribution topography of absorbed power in a discharge chamber for the cases under research. The possible extracted ion current density is evaluated under Bohm criterion.

PACS: 52.50.Dg

1. INTRODUCTION

Nuclear scanning microprobe [1] has been developed, constructed, and put into operation at the Institute of Applied Physics of National Academy of Sciences of Ukraine (IAP NASU). The microprobe resolution depends on parameters of an ion beam generated by a plasma source and on focusing ability of a probe-forming system. High resolution of a microprobe requires improved parameters (current, current density distribution and brightness) of an ion beam injected onto an input of a probe-forming system.

In nuclear scanning microprobes (NSMP) RF plasma sources are widely used as ion beams generators, since they best meet economic requirements (i.e. have a relatively small value of consumed energy) and have a sufficient operating resource. They can function in various modes: inductive, helicon, and others [1]. High efficiency of plasma generation in helicon RF sources was first revealed experimentally in works [2,3]. Still, mechanisms of high efficiency of RF power absorption in helicon sources remained unclear for a long time. Work [4] first proposes and studies a collisional heating of plasma electrons during its interaction with longitudinal Trivelpiece – Gould wave (TG wave) for a RF helicon sources.

However, work [5] draws attention to the fact that collisionless Cherenkov absorption of TG wave energy by plasma electrons may be crucial for high heating efficiency of plasma electrons for helicon sources. Thus, as dictated by the experimental conditions (a neutral gas pressure, geometry dimensions of a source etc.) one or another elementary mechanism may pre-

vail in plasma formation, or both mechanisms may play commensurable part.

The article studies spatial distribution of RF power absorbed by a plasma electron subsystem in a source discharge chamber. Geometry of a plasma ion source is close to that of IAP NASU operating with hydrogen or helium plasma. Here singly ionized ions of hydrogen and helium are considered. Ion beams are applied in an IAP NASU nuclear scanning microprobe (proton beam is for PIXE analytical technique, helium beam is for hydrogen analysis in the samples).

Known spatial distribution of absorbed power in a source discharge chamber allows evaluation of absolute integral loss of RF power that is expended for heating of a plasma electron subsystem; and variations of these distributions in relation to the source parameters (plasma density, electron temperature, value of external uniform magnetic field, geometry of a source, exiting antenna). In work [6] the TG wave was shown to be absorbed either at a surface of a plasma column or in its volume. This aspect is crucial for extraction of the beams from a plasma surface since some conditions for TG wave volume absorption should be realized in a plasma source. The article concerns TG wave absorption subject to specific parameters of an ion plasma source of the IAP NASU nuclear scanning microprobe.

Let's discuss the aims and problems of the article. Development of a complete theory on a plasma source operation with specified form of phase characteristics of an extracted ion beam is a challenge since it is related to non-stationary phenomena in an essentially

*Corresponding author E-mail address, fax, tel: oleg-alexenko@mail.ru, fax 8(0542)22-37-60, tel 8(0542)22-27-94

inhomogeneous plasma. Therefore, a separate operating stage of a plasma source is regarded here. The stage under consideration is the transmission process of RF field power to a plasma electron subsystem of an ion source and a process of plasma density increase through a mechanism of electron-neutral atom collisions at plasma-forming gas pressure of 6 mTorr, 10 mTorr. Our prime interest is in the modes where RF power of 300 W at most is absorbed inside discharge chamber. Maximum extracted density of ion current was evaluated from Bohm criterion. Such evaluation will be correct only for cases where almost whole absorbed power is concentrated in a paraxial area of the discharge chamber.

2. MODEL OF THE SOURCE

Fig.1 presents a scheme of an ion source model for consideration of theoretical and numerical solution of spatial distribution of RF power absorbed by a plasma electron subsystem inside ion source. Lateral dimensions of the model are limited by a thin cylindrical quartz discharge chamber of radius R and length L . In addition, there are conductive metal flanges placed on ends of the discharge chamber.

Permittivity tensor does not depend on z and θ coordinates, the problem may be solved when field and current of the antenna are decomposed into normal modes.

As azimuthally symmetric antenna ($m=0$) is considered here, the fields and current of the antenna are decomposed into Fourier series expansion only by z coordinate.

Alternating current of w frequency is created in the four-coil antenna by an external generator. Distance between the antenna coils is 3 mm. The second coil is placed on the $L/2$ distance from discharge chamber end.

The ion source discharge chamber and the antenna is assumed to be immersed into external uniform magnetic field with an induction \vec{B}_0 . The external magnetic field is directed along the discharge chamber axis.

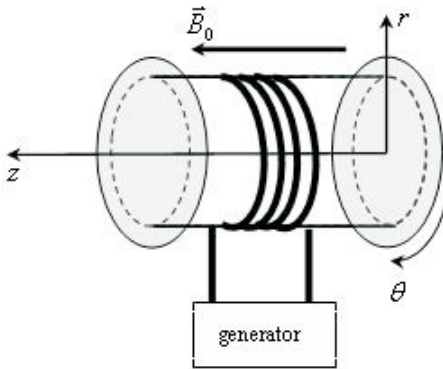


Fig.1. The ion source layout

Partially ionized electron plasma with uniform electrons and ions distribution $n_{0e} = n_{0i} = n_0$ is assumed to be previously created inside the discharge

chamber. Density of neutral atoms of gases under consideration is given by the gas pressure.

We consider the case when an external exciting frequency w is less than lower hybrid frequency w_{LH} in plasma. Plasma ions are immovable for this case.

3. ELECTROMAGNETIC FIELD, ANTENNA CURRENT AND BOUNDARY CONDITIONS. CONSIDERATION OF POWER ABSORPTION MECHANISMS

The electric and magnetic field strength satisfy the Maxwell equations with the permittivity tensor of cold magnetoactive plasma [7]. Since the condition $w < w_{LH}$ is satisfied, the permittivity tensor considers only a plasma electron subsystem:

$$\epsilon_{ik} = \begin{pmatrix} \epsilon_{\perp} & ig & 0 \\ -ig & \epsilon_{\perp} & 0 \\ 0 & 0 & \epsilon_{\parallel} \end{pmatrix}, \quad (1)$$

where:

$$\epsilon_{\perp} = 1 - \frac{w_{pe}^2}{w^2 - w_{ce}^2} + i \frac{w_{pe}^2 (w^2 + w_{ce}^2) \nu_{eff}}{w (w^2 - w_{ce}^2)^2} + i \sqrt{\frac{\pi}{8}} \frac{w_{pe}^2}{w k_z v_{Te}} \left[\exp\left(-\frac{(w - w_{ce})^2}{2k_z^2 v_{Te}^2}\right) + \exp\left(-\frac{(w + w_{ce})^2}{2k_z^2 v_{Te}^2}\right) \right],$$

$$g = \frac{w_{pe}^2 w_{ce}}{w (w^2 - w_{ce}^2)} + i \frac{2w_{pe}^2 w_{ce} \nu_{eff}}{(w^2 - w_{ce}^2)^2} +$$

$$i \sqrt{\frac{\pi}{8}} \frac{w_{pe}^2}{w k_z v_{Te}} \left[\exp\left(-\frac{(w - w_{ce})^2}{2k_z^2 v_{Te}^2}\right) - \exp\left(-\frac{(w + w_{ce})^2}{2k_z^2 v_{Te}^2}\right) \right],$$

$$\epsilon_{\parallel} = \epsilon' + i(\epsilon''_{CL} + \epsilon''_{LAN}),$$

$$\epsilon_{\parallel} = 1 - \frac{w_{pe}^2}{w^2} + i \frac{w_{pe}^2 \nu_{eff}}{w^3} + i \sqrt{\frac{\pi}{2}} \frac{w_{pe}^2 w}{k_z^3 v_{Te}^3} \exp\left(-\frac{w^2}{2k_z^2 v_{Te}^2}\right),$$

$$w_{LH} \approx \sqrt{w_{ce} w_{ci}}; \quad w_{pe}^2 = \frac{n_0 e^2}{m_e \epsilon_0}; \quad w_{ce} = \frac{e B_0}{m_e}; \quad w_{ci} = \frac{e B_0}{m_i}.$$

Relation between electric induction vector and vector of electric field strength is described by constitutive equation:

$$\vec{D} = \epsilon(w) \vec{E}. \quad (2)$$

Anti-Hermitian part of the dielectric tensor considers two mechanisms of electromagnetic wave absorbed by the plasma electron subsystem that are collisional and collisionless. The collision mechanism depends on effective frequency of electron collision with neutral atoms and with generated ions of gases under consideration.

At electron temperature of 5 eV and pressure of plasma forming gas of 1 mTorr, "electron-neutral" collision frequency is 2,7 MHz for helium plasma and 4,7 MHz for hydrogen plasma.

"Electron-ion" Coulomb collisions are calculated with allowance of averaging over Maxwellian distribution function of electron velocity:

$$\nu_{eff} = \nu_{en} + \nu_{ei}. \quad (3)$$

Collisionless mechanism depends on external disturbance frequency w , length L of a discharge chamber, plasma density n_0 and temperature T_e of electron plasma component T_e .

This article discusses the cases for hydrogen and helium at $k_z = \pi/L$, $f = 27,12$ MHz where the basic heating mechanism of plasma electron subsystem is collisional. Collisionless heating mechanism introduces negligible corrections and we do not consider it in our calculations.

The graphs below represent estimate correlation of two mechanisms of power absorption in the tensor component ϵ_{\parallel} . Figs.2,a and 3,a represent the data for chamber length $L = 6cm$. Figs.2,b and 3,b represent the data for chamber length $L = 7cm$. The ratio $\epsilon''_{LAN}/\epsilon''_{CL}$ is is showed on the graphs in numbers.

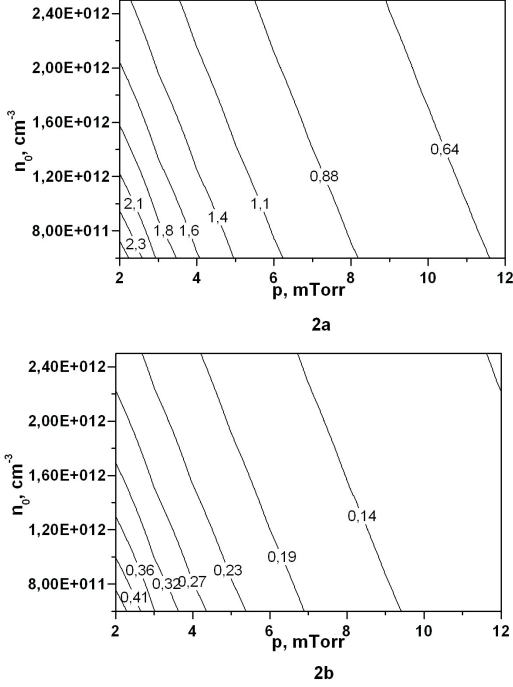


Fig.2. Influence of two mechanisms of power absorption. Plasma-forming gas is helium, $k_z = \pi/L$, $f = 27,12$ MHz

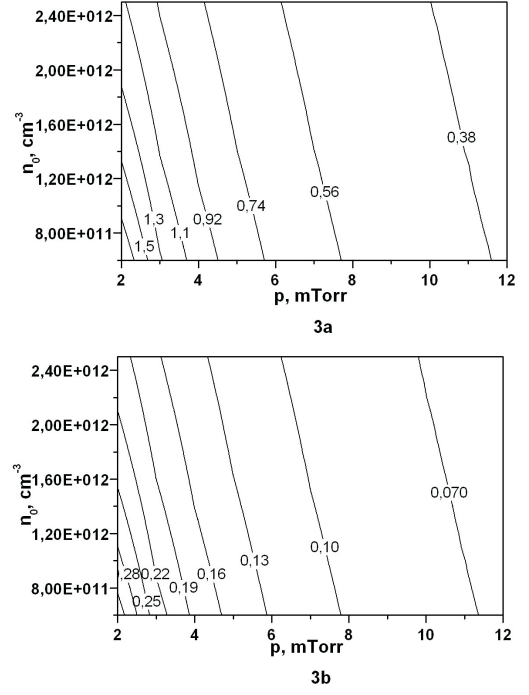


Fig.3. Influence of two mechanisms of power absorption. Plasma-forming gas is hydrogen, $k_z = \pi/L$, $f = 27,12$ MHz

In our case a collisionless mechanism is seen to develop itself significantly for chambers with $L = 6cm$ or less. Tangential components of electric field are continuous at the “plasma–vacuum” interface:

$$E_z^{pl} = E_z^{vac}, E_{\theta}^{pl} = E_{\theta}^{vac}. \quad (4)$$

Tangential components of magnetic field are discontinuous at the “plasma–vacuum” interface because of antenna current flow:

$$H_z^{pl} - H_z^{vac} = -j_{\theta}, H_{\theta}^{pl} = H_{\theta}^{vac}. \quad (5)$$

The field components and antenna current are found in the Fourier series form since discharge chamber is limited along the z axis:

$$\vec{j}_{\theta} = \sum_n \vec{e}_{\theta} j_{\theta}(r) \sin(k_{zn}z), \quad (6)$$

$$\vec{E} = \sum_n \vec{e}_r E_r(r) \sin(k_{zn}z) + \vec{e}_{\theta} E_{\theta}(r) \sin(k_{zn}z) + \vec{e}_z E_z(r) \cos(k_{zn}z), \quad (7)$$

$$\vec{H} = \sum_n \vec{e}_r H_r(r) \cos(k_{zn}z) + \vec{e}_{\theta} H_{\theta}(r) \cos(k_{zn}z) + \vec{e}_z H_z(r) \sin(k_{zn}z), \quad (8)$$

where $k_{zn} = n\pi/L$, n is a longitudinal harmonic number; L is a discharge chamber length.

Here tangential components of electric field are equal to zero at metal ends of the discharge chamber. Fourier amplitudes of current density in a 4– coil antenna have a form of:

$$j_{\theta} = \frac{I_A}{L} \delta(r - r_A) \sin(k_{zn}z_A), \quad (9)$$

where: I_A is a current amplitude in Amperes; z_A is a coil coordinate along the axis; r_A is a radius of the antenna, and it is equal R .

Explicit form of the electromagnetic field components is obtained in the usual way [8] and is not given here as cumbersome.

Boundary conditions and Maxwell equations in coordinate axes projections are written for Fourier

amplitudes of field component and for Fourier amplitudes of antenna current density.

With known explicit expression for components of electromagnetic field inside the discharge chamber, RF power integral absorption in the discharge chamber may be calculated:

$$P_{abs} = \frac{w\epsilon_0}{2} \iiint_V \text{Im} \left[\epsilon_{\perp} \left(|E_r|^2 + |E_{\theta}|^2 \right) + \epsilon_{\parallel} |E_z|^2 + ig \left(E_{\theta}^* E_r - E_r^* E_{\theta} \right) \right] dV.$$

The expression under integral defines a spatial distribution of the RF power absorption.

4. NUMERICAL CALCULATIONS AND DISCUSSION

Numerical calculations were done for helium and hydrogen, and a discharge chamber of a 1,5 cm radius, 7 cm and 12 cm length. Other parameters were antenna current of 3,5 A, plasma forming gas pressure of 6 mTorr or 10 mTorr, electron temperature of 5 eV, ion temperature of 0,1 eV.

The mode of the ion source with electromagnetic wave exited inside the discharge chamber with $k_z = \pi/L$ is considered here.

For a wave with $k_z = \pi/L$ to be exited the second coil of the antenna should be placed in the middle of the discharge chamber length.

Before calculations the transparency diagrams are plotted under [6] criteria for helicon waves and Trivelpiece – Gould waves (Figs.4,5), for two discharge chambers under investigation. The articles [4, 5, 6, 7] represent that the helicon wave and TG wave exists together in the helicon plasma source with a dielectric discharge chamber and cannot be separated in the discharge chamber.

In other words, there is a hybrid TG + helicon mode propagated in the helicon plasma source with a dielectric discharge chamber.

In reference to the above, the regions of common existence of helicon and TG wave are of practical concern at the transparency diagrams. The power absorption resonances would be searched only at these regions. The diagram regions where only a TG wave exists are of no interest since in real experiment it is impossible to excite only TG wave in a helicon plasma source with a dielectric chamber.

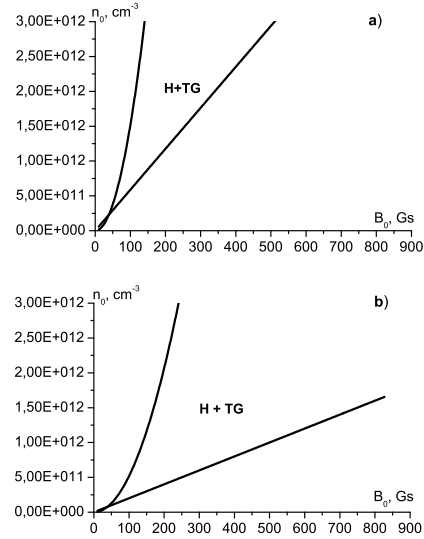


Fig.4. Wave transparency regions. Plasma-forming gas is helium. a) discharge chamber with $L=7$ cm; b) discharge chamber with $L=12$ cm

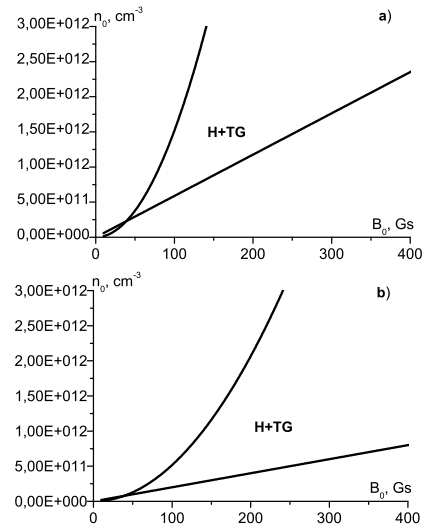


Fig.5. Wave transparency regions. Plasma-forming gas is hydrogen. a) discharge chamber with $L=7$ cm; b) discharge chamber with $L=12$ cm

The graphs (Figs.6–9) give information on plasma density values of resonant RF – power input kept for helium and hydrogen plasma.

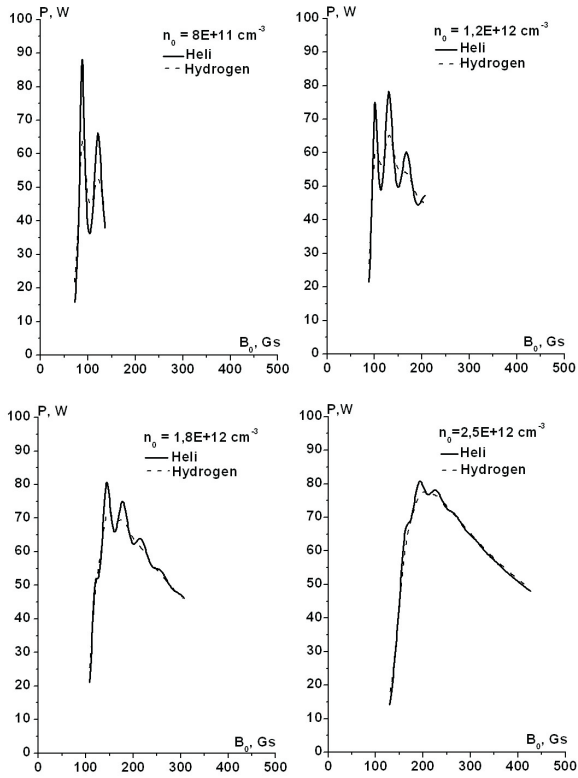


Fig. 6. Power absorption for a discharge chamber with $L=7$ cm at 6 mTorr pressure

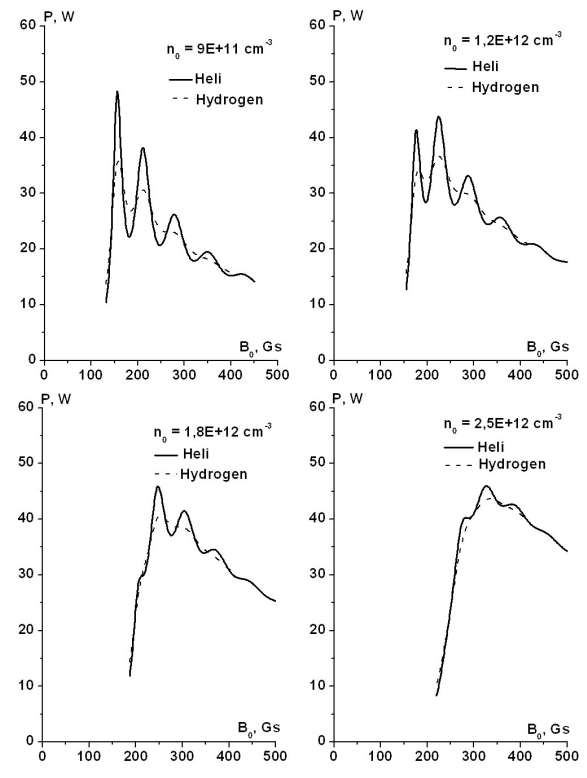


Fig. 8. Power absorption for a discharge chamber with $L=12$ cm at 6 mTorr pressure

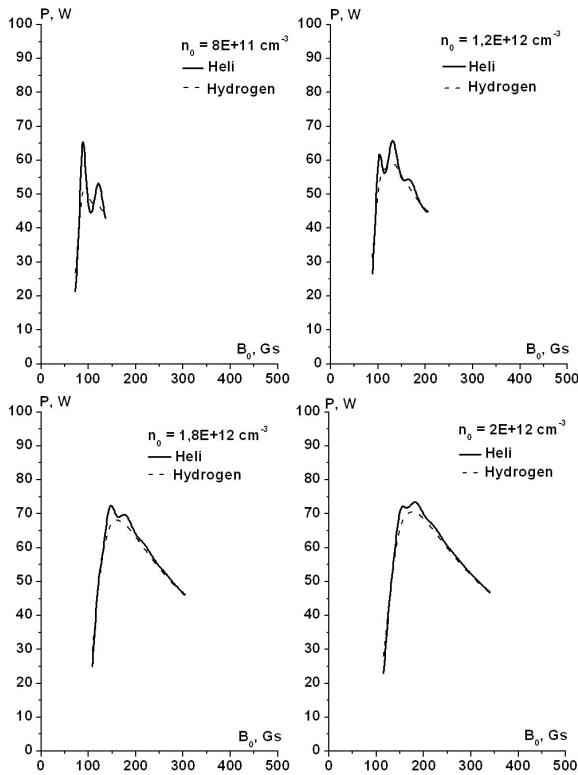


Fig. 7. Power absorption for the discharge chamber with $L=7$ cm at 10 mTorr pressure

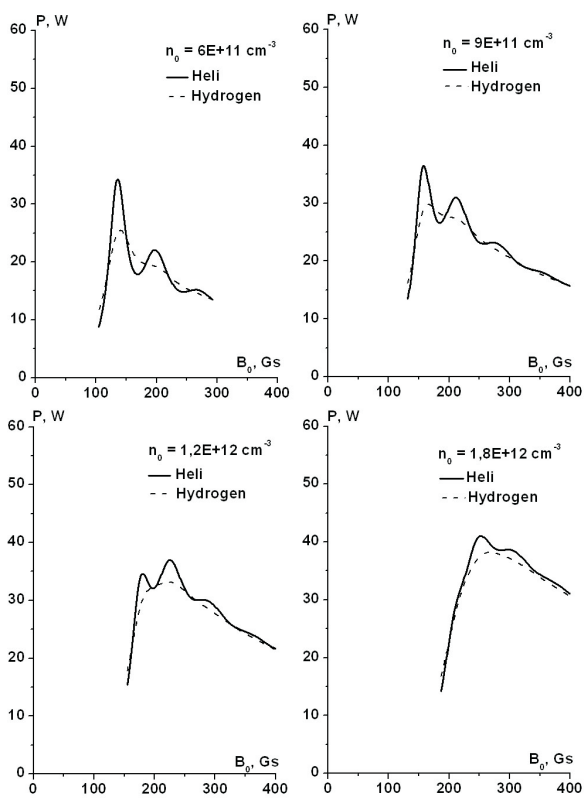


Fig. 9. Power absorption for a discharge chamber with $L=12$ cm at 10 mTorr pressure

This information can be conveniently represented in a tabulated form.

Gas	Chamber length, cm	Gas pressure, mTorr	Plasma density, cm^{-3}
hydrogen	7	6	1.2E+12
helium	7	6	2.5E+12
hydrogen	12	6	1.2E+12
helium	12	6	2.5E+12

Gas	Chamber length, cm	Gas pressure, mTorr	Plasma density, cm^{-3}
hydrogen	7	10	8E+11
helium	7	10	1.8E+12
hydrogen	12	10	8E+11
helium	12	10	1.8E+12

Analysis of a 3D distribution of power absorption at resonances (Figs.6–9) shows that these resonances are not equivalent with relation to power distribution in a discharge chamber.

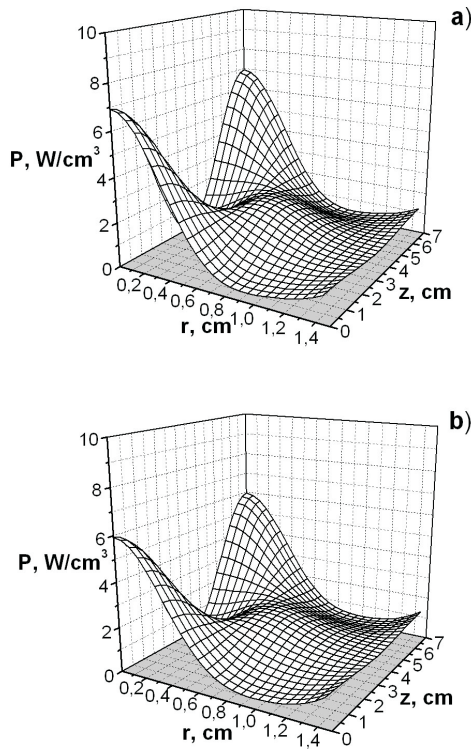


Fig.10. Discharge chamber with $L=7$ cm, $p=6$ mTorr, at plasma density $n_0 = 1,2E + 12$ cm^{-3} . 10a) helium plasma, $B_0 = 102$ Gs, 10b) hydrogen plasma, $B_0 = 104$ Gs

For helium plasma, with gas pressure of 6 mTorr and 10 mTorr at both chambers, penetration of absorbed power into the paraxial region (Figs.10–13) is better at resonance with plasma density of $1,2E + 12$ cm^{-3} than at resonance with plasma density of $1,8E + 12$ cm^{-3} ... $2,5E + 12$ cm^{-3} . Maximum density of extracted ion current at plasma density of $1,2E + 12$ cm^{-3} for helium plasma is $J_+ = 120$ mA/cm².

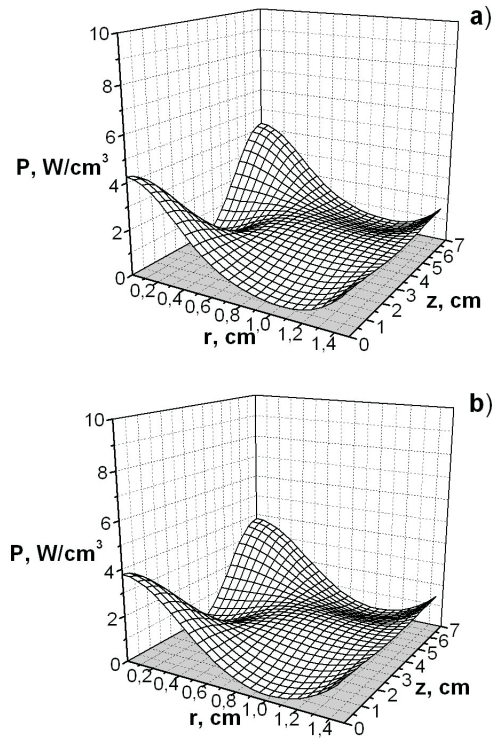


Fig.11. Discharge chamber with $L = 7$ cm, $p = 10$ mTorr, at plasma density $n_0 = 1,2E + 12$ cm^{-3} . 11a) helium plasma at $n_0 = 1,2E + 12$ cm^{-3} , $B_0 = 107$ Gs, 11b) hydrogen plasma at $n_0 = 8E + 11$ cm^{-3} , $B_0 = 92$ Gs

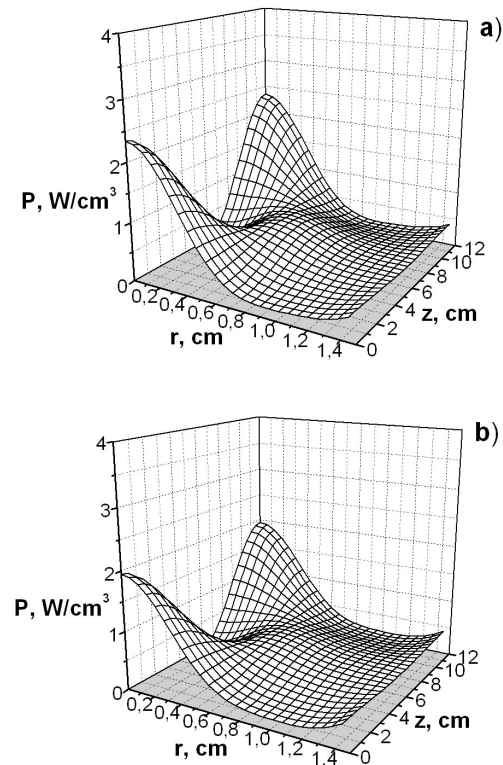


Fig.12. Discharge chamber with $L = 12$ cm, $p = 6$ mTorr, at plasma density $n_0 = 1,2E + 12$ cm^{-3} . 12a) helium plasma, $B_0 = 179$ Gs, 12b) hydrogen plasma, $B_0 = 182$ Gs

For hydrogen plasma, with gas pressure of 6 mTorr at both chambers, penetration of absorbed power into the paraxial region (Figs.10–13) is better at resonance with plasma density of $1,2E + 12 \text{ cm}^{-3}$; $J_+ = 238 \text{ mA/cm}^2$ than at resonance with plasma density of $1,8E + 12 \text{ cm}^{-3} \dots 2,5E + 12 \text{ cm}^{-3}$; with gas pressure of 10 mTorr, penetration of absorbed power is better at resonance with plasma density of $8E + 11 \text{ cm}^{-3}$; $J_+ = 159 \text{ mA/cm}^2$.

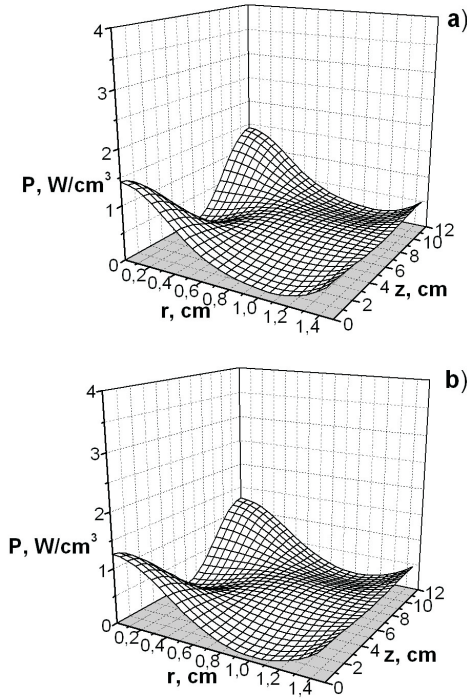


Fig.13. Discharge chamber with $L = 12 \text{ cm}$, $p = 10 \text{ mTorr}$, at plasma density $n_0 = 1,2E + 12 \text{ cm}^{-3}$. 13a) helium plasma at $n_0 = 1,2E + 12 \text{ cm}^{-3}$, $B_0 = 184 \text{ Gs}$, 13b) hydrogen plasma at $n_0 = 8E + 11 \text{ cm}^{-3}$, $B_0 = 158 \text{ Gs}$

5. CONCLUSIONS

Experimental results from [9] are compared with theoretic calculations obtained here.

According to the experiment [9], density of helium plasma $n_0 = 9E + 11 \text{ cm}^{-3}$ is achieved at 225 W in plasma of a helicon source. The extracted ion current has a value 90 mA/cm^2 here.

Balance of power may be theoretically estimated with the technique described in [10].

For plasma parameters $n_0 = 9E + 11 \text{ cm}^{-3}$, $p = 10 \text{ mTorr}$, and discharge chamber parameters $R = 1,5 \text{ cm}$, $L = 12 \text{ cm}$ the results are obtained as follows:

1) power carried out by electrons onto the discharge chamber walls is defined by expression:

$$P_e = n_0 \cdot u_B \cdot S \cdot \epsilon_e,$$

where:

n_0 is a plasma density;

u_B is a Bohm velocity of the ions;

S is a lateral surface area of the discharge chamber;

ϵ_e is the energy carried by single electron out of the discharge;

$$\epsilon_e = 2T_e,$$

$$P_e = 201 \text{ W};$$

2) power carried out by ions onto the discharge chamber walls is defined by expression:

$$P_i = n_0 \cdot u_B \cdot S \cdot \epsilon_i,$$

where ϵ_i is the energy carried by a single ion out of the discharge;

$$\epsilon_i = 0,5T_e + T_e \cdot \ln\left(\frac{M_i}{2 \cdot \pi \cdot m_e}\right)^{1/2}$$

$$P_i = 28,6 \text{ W};$$

3) power, consumed for heating of electron plasma component by pair collisions, may be defined on Fig.9 as 33 W (first resonance).

Therefore, as to theoretical data, minimum power required for RF discharge maintenance is 263 W. Density of maximum extracted ion current is theoretically esteemed to be $89,5 \text{ mA/cm}^2$ according to Bohm criterion.

Theoretical data are seen to be in a good agreement with experimental data witnessing reasonable adequacy of the plasma source model used.

References

1. S.M. Mordyk, V.I. Voznyy, V.I. Miroshnichenko, V.E. Storizhko, B. Sulkio-Cleff, D.P. Shulha. Hydrogen/helium ion injector for accelerator – based microprobe facilities // *Nuclear Instruments and Methods in Physics Research*. 2006, v. B231, p. 37–42.
2. R.W. Boswell. Plasma production using a standing helicon wave // *Physics Letters*. 1970, v. 33A.
3. R.W. Boswell. Very efficient plasma generation by whistler waves near the lower hybrid frequency // *Plasma Physics and Controlled Fusion*. 1984, v. 26, N10, p. 1147–1162.
4. K.P. Shamrai, V.B. Taranov. Resonance wave discharge and collisional energy absorption in helicon plasma source // *Plasma Phys. Control. Fusion*. 1994, v. 36, p. 1719–1735.
5. А.Ф. Александров, Н.Ф. Воробьев, Е.А. Кралькина, В.А. Обухов, А.А. Рухадзе. Теория квазистатических плазменных источников // *Журнал технической физики*. 1994, т. 64, вып. 11 (in Russian).

6. K.P. Shamrai, V.B. Taranov. Volume and surface rf power absorption in a helicon plasma source // *Plasma Sources Sci. Technol.* 1996, v. 5, p. 474–491.
7. А.Ф. Александров, Г.Е. Бугров, К.В. Вавилин, И.Ф. Керимова, С.Г. Кондранин, Е.А. Кралькина, В.Б. Павлов, В.Ю. Плаксин, А.А. Рухадзе. Самосогласованная модель ВЧ индуктивного источника плазмы, помещенного во внешнее магнитное поле // *Физика плазмы.* 2004, т. 30 (in Russian).
8. Я.Б. Файнберг, М.Ф. Горбатенко. Электромагнитные волны в плазме, находящейся в магнитном поле // *Журнал технической физики.* 1959, т. XXIX, вып. 5. (in Russian).
9. С.Н. Мордик, В.И. Возный, В.И. Мирошниченко, А.Г. Нагорный, Д.А. Нагорный, В.Е. Сторижко, Д.П. Шульга. Геликонный источник ионов в режиме высокой плотности плазмы // *Вопросы атомной науки и техники.* 2006, №5, с. 208–211 (in Russian).
10. M. A. Lieberman, and A. J. Lichtenberg. Principles of Plasma Discharge and Material Processing // ISBN 0-471-72001-1 Copyright 2005 John Wiley and Sons, Inc.

РЕЗОНАНСНИЙ ВВОД ВЧ-ЭЛЕКТРОМАГНИТНОГО ПОЛЯ В ПЛАЗМЕННОМ ИОННОМ ИСТОЧНИКЕ ГЕЛИКОННОГО ТИПА

О. В. Алексенко, В. И. Мирошниченко, С. Н. Мордик

Исследуется пространственное распределение поглощения ВЧ-электромагнитного поля электронной подсистемой плазмы источника. Источник ионов работает в геликонном режиме ($w_{ci} < w < w_{ce} < w_{pe}$). Для исследований используется упрощенная модель плазменного ВЧ – источника. Расчеты проводились для двух конкретных геометрических размеров разрядной камеры в предположении возбуждения симметричных мод при двух различных значениях давления рабочего газа – гелия, водорода. Для расчетов выбраны параметры источника ионов инжектора ядерного сканирующего микроскопа ИПФ НАН Украины. Результаты численного счета показывают резонансный характер интегрального поглощения ВЧ мощности в зависимости от значения величины магнитного поля при фиксированной плотности плазмы. Острота резонансов уменьшается с ростом давления рабочего газа. Приводится топография распределения величины поглощаемой мощности внутри объема разрядной камеры для рассмотренных случаев. На основании критерия Бома делается оценка значения плотности возможного извлекаемого ионного тока.

РЕЗОНАНСНИЙ ВВОД ВЧ-ЭЛЕКТРОМАГНИТНОГО ПОЛЯ В ПЛАЗМОВОМУ ІОННОМУ ДЖЕРЕЛІ ГЕЛІКОННОГО ТИПУ

О. В. Алексенко, В. И. Мирошниченко, С. М. Мордик

Досліджується просторовий розподіл поглинання ВЧ-електромагнітного поля електронною підсистемою джерела. Джерело іонів працює в геліконному режимі ($w_{ci} < w < w_{ce} < w_{pe}$). Для досліджень використано спрощену модель плазмового ВЧ-джерела. Розрахунки проводились для двох конкретних геометричних розмірів розрядної камери в припущенні збудження симетричних мод при двох різних значеннях тиску робочого газу – гелію, водню. Для розрахунків обрано параметри джерела іонів інжектора ядерного скануючого микроскопа ІПФ НАН України. Результати чисельного розрахунку показують резонансний характер інтегрального поглинання ВЧ потужності в залежності від значення величини магнітного поля при фіксованій густини плазми. Гострота резонансів зменшується з ростом тиску робочого газу. Наведено топографію розподілу величини потужності, що поглинається всередині об'єму розрядної камери, для розглянутих випадків. На підставі критерію Бома зроблено оцінку значення густини можливого екстрагуємого іонного струму.